Int. J. Bio-Inorg. Hybr. Nanomater., 10(4): 233-248, Winter 2021

A Theoretical study of the effects of different solvents on the connections of methotrexate anticancer drug to carbon nanotubes carriers: AQM.MM study

V. Khodadadi[1], N. Hasanzadeh[2], H. Yahyaei[3,] & A. Rayatzadeh[4]*

[1,2,4] *Department of Chemistry, Ahvaz Branch, Islamic Azad University, Ahvaz, Iran*
[3] *Department of Chemistry, Zanjan Branch, Islamic Azad University, Zanjan, Iran*

Received: 8 June 2021; Accepted: 11 August 2021

ABSTRACT: In this investigation, the interaction of methotrexate anticancer drug (MTX) with single-wall carbon nanotubes (SWNTs) and double-wall carbon nanotubes (DWNTs) was examined via AMBER, OPLS, CHARMM and MM+ force fields through the molecular mechanic (MM) method. The calculations were performed out by the Monte Carlo simulation method at different temperatures. Using the mentioned force fields, we investigated the effects of gas-phase and various solvent media with different dielectric constants, i.e., water, DMSO, methanol, ethanol and DMF at ten different temperatures on the interaction of MTX with DWNTs. The interaction of MTX, with SWNTs and DWNTs in the gas phase has been processed using the DFT calculations. Thus, by utilizing a DFT method, we studied the effects of different solvents on the interaction of MTX, with carbon nanoparticles within the Onsager self-consistent reaction field (SCRF) model, as well as the effects of temperature on the stability of the interaction between compounds in various solvents. Frontier molecular orbitals (FMOs), total density of states (DOS), thermodynamic parameters and molecular electrostatic potentials (MEP) of the title compounds were investigated by theoretical calculations. Molecular properties such as the ionization potential (I), electron affinity (A), chemical hardness (η), electronic chemical potential (μ) and electrophilicity (ω) were investigated for the structures. The major finding is that the Monte Carlo and Molecular mechanics-quantum mechanics results for thermodynamic properties and conformer populations are in accord.

Keywords: *Double-wall carbon nanotubes (DWNTs); Force field; Methotrexate anticancer drug; Monte Carlo simulation; Single-wall carbon nanotubes (SWNTs).*

INTRODUCTION

Carbon nanotubes (CNT) possess extraordinary properties. Hence, they are unique nano systems. In such nanotubes, carbon atoms are interconnected through covalent bonds. Carbon nanotubes (CNT) include single-walled nanotubes (SWNTs) and multi-walled nanotubes (MWNTs) [1-3]. MWNTs can only have semiconductor behavior, but SWNTs can act as metallic or semiconductor conductors. SWNTs are considered as one of the most suitable items for being used in biological systems due to their appropriate size, biocompatibility, controllable properties and the ability to have reversible responses compared to biochemicals.

(*) Corresponding Author - e-mail: Hooriye_Yahyaei@yahoo.com

For instance, SWNTs can easily pass through the shell and biological barriers and enter the cell because of their small size; they have a diameter about half of that of a DNA strand [4, 5]. The applications of nanotubes and their use as drug nano-carriers have received much attention recently [6, 7]. In particular, functional drug-containing nanotubes (drug nano-carriers) have helped develop a new generation of drugs and have created a new chapter of treatment in medical science [8, 9]. Conducted investigations have proved that carbon nanotubes are not inherently toxic. Therefore, these nanotubes can be a suitable option for being used as carrier nanotubes and drug delivery [10, 11]. Research has demonstrated that due to the permeability of veins in cancerous tissues, drug nano-carriers can penetrate tumor masses and increase the density of nano drugs in the tumor [12, 13]. Drug nano-carriers are capable of improving the treatment through controlling the drug release, increasing the half-life of the drug and increasing the drug density; on the other hand, they are able to reduce the detrimental effects of chemical toxicity of drugs by decreasing drug density in the healthy parts of the body [14]. Recently, numerous instances of drug delivery systems which benefit from nanotechnology for treating cancer have been investigated [15].

In our case, research has focused on the molecule of methotrexate drug embedded in single-walled and double-walled nanotubes. Methotrexate (MTX), also known as Rheumatrex and Trexall, is a drug used to treat a variety of cancers, such as acute leukemia and to counteract a variety of tumors [16-19]. Several pharmacological mechanisms of methotrexate have been proposed, including inhibition of purine and pyrimidine synthesis, suppression of methylation transfer reactions by polyamine accumulation, reduction of antigen-dependent T cell proliferation, and promotion of adenosine release by adenosine-mediated suppression of inflammation [20]. Research has revealed that methotrexate affects cancer by inhibiting the enzyme involved in the production of tetrahydrofolate or dihydrofolate reductases [21-23]. It operates in a way that, the enzyme dihydrofolate reductase and coenzyme NADPH + H, restores.reduces the dihydrofolate and catalyzes the tetrahydrofolate, which is a major cofactor in the production of thymidine, RNA and DNA [24-26].

Research has demonstrated have proved that tubular particles are able to enter the cell faster than other particles [27]. They have also demonstrated that the controlled release of MTX in non-spherical nanoparticles is higher and more effective and that it occurs slowly in treating cancer treatment. Therefore, drug nanoparticles have better therapeutic efficacy in comparison to spherical nanoparticles with tubes [28-30]. Nowadays, designing and simulating medicine with the help of computers and specialized software have become particularly important [31]. Through this method, it is possible to save time and money on developing new drugs by identifying the drug molecule and the receptor in the body and using techniques that evaluate the interaction of these compounds in the same environment [32, 33]. The use of computational methods plays an important role in improving the understanding and optimization of laboratory processes to evaluate the drug delivery capability of drug carriers. Computational simulation, which employs computational chemistry software used in pre-laboratory research to produce more effective drugs with less side effects, can lead to faster and more cost-effective prognosis, diagnosis and treatment in cancer patients [34, 35].

In the present study, by using advanced software such as Hyper compact, structural, thermo-dynamic and electronic information for single-walled and double-walled methotrexate anticancer drug complexes have been presented using quantum and Monte Carlo calculations as well as and molecular mechanics over a range of temperatures and solvents [36, 37]. Thus, by comparing the energies computed through Monte Carlo calculations in the CHARMM, AMBER, MM + and OPLS force fields, the differences in the complexes resulting from the incorporation of the methotrexate drug molecule into single-walled nanotubes (SWNTs) and double-walled nanotubes (DWNTs) are demonstrated [38, 39]. It should also be noted that in addition to investigating the interaction effects of methotrexate with SWNTs and DWNTs, the interaction of MTX and SWNTs in the gas phase as well as in the solvents DMF, DMSO, water, ethanol and methanol has been studied using different force fields and Monte Carlo calculations; the same procedure was followed for the interaction between MTX and

DWNTs. It is evident that the formation of a stable MTX complex with SWNT and also MTX with nanotubes is of prime importance.

COMPUTATIONAL METHOD

In this study, the calculations related to the interaction between methotrexate anticancer drug and single wall carbon nanotubes (SWNTs) and double wall carbon nanotubes (DWNTs) have been carried out using each of the force fields (AMBER, OPLS, CHARMM and MM+). This method is utilized in HyperChem software. Four different force fields are available in the macro model program. Choosing a force field that is well parameterized for the molecular system under study is very important [40, 41]. Monte Carlo simulation is a useful tool for areas which are difficult or cumbersome to study using experimental approaches, and it simultaneously offers fundamental insights on the underlying physics of the simulated system on a micro/nanoscale [42-44]. The essential step for the successful use of Monte Carlo simulations is the development of a reliable force field, which is responsible for capturing relevant molecular interactions. Accurate force fields are required to reproduce the dynamic and static properties of a system. Furthermore, an important requirement for molecular studies of compounds in the solvent is the correct description by the force field. Classical force fields contain empirically based interatomic potentials to compute the energy between atoms based on their positions. The classical approximation is well-suited for noncovalent interactions between atoms, such as Coulombic, van der Waals, and angle-strain interactions [45]. In this investigation, differences in force fields are illustrated by comparing the energies calculated using force fields AMBER, OPLS, CHARMM and MM+. In this study, HyperChem professional release 7.01 is used for the molecular mechanics calculations. Geometry optimization as well as Monte Carlo simulation were performed using this software [11]. The quantum chemical calculations were performed using the Gaussian 09W software [46]. The molecular structure of the title compounds in the ground state was optimized using the Density Functional Theory (DFT/B3LYP/6-31+G*) [47]. The Polarized Continuum Model (PCM) [48], The Frontier Molecular Orbital (FMO) analysis and electronic properties such as energies HOMO and LUMO orbitals, HOMO-LUMO energy gap (Eg), ionization potential (I), electron affinity (A), global hardness (η), electronegativity (χ), electronic chemical potential (μ), electrophilicity (ω) and chemical softness (S) were estimated through the E_{HOMO} and E_{LUMO} energies using the B3LYP/6-31+G* level of theory [49, 50].

The optimized molecular structures, Molecular Electrostatic Potential (MEP) maps and UV-Vis spectra were visualized using GaussView 05 program [47]. There are three types of QMC: variation, diffusion and green's functions. These methods act with an openly correlated wave function and calculate integrals numerically, utilizing a Monte Carlo integration. These calculations are very time consuming, but they are the most accurate methods known to date. Overall, DFT calculations provide perfect and increasingly more accurate quantitative results as the molecules under consideration become smaller [51]. DFT methods are accessible in macro model programs as well. Choosing a level that is well-parameterized for the molecular system under investigation is important. Conformational interconversions are governed by precise energy parameters and geometry coordinates, which are vital in molecular systems, too. Low-energy structures found on each surface were chosen and exposed to unrestrained quantum mechanical minimization through B3LYP/6-31+G* SCRF [52].

RESULTS AND DISCUSSION

In the present study, calculations related to the interaction between methotrexate anticancer drug and Single Wall and Double Wall carbon nanotubes (SWNTs & MWNTs) have been carried out using AMBER, OPLS, CHARMM (BIO+) and MM+ force fields. Biomolecules are complex systems. Their structures are represented by multidimensional rugged energy landscapes with a huge number of local minima separated by high energy barriers. Thus, any simulation study primarily deals with adequate description of the atomistic interaction or force field and convergence of

the configuration space sampling of such a complex energy landscape. Efficient sampling can be achieved through enhanced conformational search techniques. The experimental values of the properties predicted by a force field are signs of its quality. There are four predominantly used force field families for molecular mechanic simulations at the time, including AMBER, OPLS, CHARMM (BIO+) and MM+ [53, 54]. These classic force fields have constantly been improved and verified; however, given the intricacies of the energy landscape, the successful applications of these fields in many systems remain to be validated. Thus, how the employed force field affects the simulation results is a question worth investigating [55].

Among other appropriate tools for evaluating probability distributions are Monte Carlo algorithms. Due to their tendency to sample low energy regions of conformational spaces, Monte Carlo-based algorithms are highly useful in finding important conformations of flexible biomolecules. With small adjustments, a Monte Carlo program can calculate a histogram of a distance distribution for a particle in harmonic potential. Such histograms illustrate that at any given temperature, the methotrexate anticancer drug atoms with carbon nanotube distance adopt a range of values. It is also observed that the range of values gets broader with the temperature, indicating increased amplitude of motion of atoms at higher temperatures [56, 57].
The effect of different solvents and temperatures on single wall carbon nanotubes (SWNTs) and double wall carbon nanotubes (DWNTs) were studies through quantum mechanics calculations and molecular mechanic simulation. Differences in force fields were illustrated by comparing the energies calculated using AMBER, OPLS, CHARM (Bio+) and MM+ force fields. The quantum mechanics (QM) calculations were carried out with the GAUSSIAN98 program based on B3LYP/6-31+G* level.

The Gaussian program employs a simple approximation in which the volume of the solute is used to compute the radius of a cavity which forms the hypothetical surface of the molecule. The structures were calculated in gas phase and in various solvent media with different dielectric constants (water (ε = 78.39), DMSO (ε = 46.8), methanol (ε = 32.63), ethanol (ε = 24.55), CH_2Cl_2 (ε = 8.93) and DMF (ε = 39.8)) at ten temperatures using a density functional theory method (DFT) at the B3LYP/6-31+G* level, the structure of double wall carbon nanotubes (DWNTs) and relative energies have has been investigated through molecular mechanics simulations and quantum mechanics calculations within the Onsager self-consistent reaction field (SCRF) model; moreover, the structural stability of the investigated nanotube has been compared and analyzed in different solvent media and at different temperatures (between 298K and 316K) [58, 59]. Since the Onsager model can conveniently describe the interaction between a molecule in a solution and its medium, we have assumed that the solute is placed in a spherical cavity inside the solvent. The latter is described as a homogeneous, polarizable medium of dielectric constant. The results of Onsager model calculations are displayed using the energy difference between these conformers, which are highly sensitive to the polarity of the surrounding solvent [60]. The solvent effect has been calculated through the SCRF model. Using this method, the Total (E_{Tot}), Potential (E_{Pot}) and Kinetic (E_{Kin}) energies (kcal/mol) were calculated for the native structure through Monte Carlo simulation in different solvents and in AMBER, OPLS, CHARMM (Bio+) and MM+ force fields, and the results have been listed in Tables 1 to 4. Tables 1-4 & Fig. 1 show the EKin changes (kcal/mol) calculated versus temperature at different dielectric constants (water (ε = 78.39), DMSO (ε = 46.8), methanol (ε = 32.63), ethanol (ε = 24.55) and DMF (ε = 39.8) through Monte Carlo simulation in the four force fields (AMBER, OPLS, CHARMM (Bio+) and MM+). The results of Monte Carlo calculations (Tables 1-4 & Fig. 1) indicate that in the gas phase, methotrexate connected to SWNTs is the most stable and has the lowest amount of energy while in the Amber force field [53, 61].

The methanol solvent displayed the lowest amount of energy and proved to be the most stable solvent for the simulation when methotrexate connected to SWNTs was simulated in water, DMSO, methanol, ethanol and DMF solvents. Similar results have been reported for OPLS and CHARMM force fields. The calculations related to the MM+ force field produced a notable result though. In the MM+ field, water is the most stable and the most suitable among the afore-

mentioned solvents for simulation, since it has the lowest amount of energy. No doubt this is positively related to the dielectric constant of the solvents. Water has the highest dielectric constant; therefore, it is considered to be the most suitable solvent for methotrexate connected to SWNTs (as seen Fig. 1) [62].

Substances with high dielectric constants are easily polarized. Polarization allows countercharges to be placed around an ion resulting in coulombic interactions between the solvent and the ion, which in turn promote solubilization of the ion through competing with interionic interactions. In a similar vein, a polar solvent–one with a high dielectric constant – will form stabilizing interactions with the solute that compete with solute-solute interactions, thereby solubilizing polar molecules. The dielectric constant of the solvent also affects the interactions in the solution that involve ions and polar molecules, decreasing the intermolecular energy as the dielectric constant increases [63, 64].

Single-wall and double-wall nanotubes are quite similar in terms of characteristics and morphologies; however, DWNTs are highly more resistant to chemicals. This feature proves to be extremely important when functionality necessitates adding new properties to the nanotube. Double-walled carbon nanotubes are coaxial nanostructures that consist of exactly two single-walled carbon nanotubes, one nested in another. This distinctive structure presents opportunities for better understanding the carbon nanomaterials family and for making greater use of it. Double-walled carbon nanotubes (DWNTs) are a new class of carbon nanostructures. A DWNT consists of exactly two concentric carbon nanotubes. This double-wall structure makes DWNTs the simplest system for investigating the effects inter-wall coupling might have on the physical properties of carbon nanotubes (CNTs). DWNTs have higher mechanical strength and thermal stability than SWNTs; in addition, they have intriguing electronic and optical features [65].

It is noteworthy that Fig. 2, (the results for methotrexate connected to DWNTs), show that the results are highly consistent with those related to methotrexate connected to SWNTs; in the force fields AMBER, OPLS and CHARMM, methanol is the most stable solvent and in the MM+ field, water is the most stable solvent [66]. On the other hand, water is a biological solvent and acts as the main foundation for chemical reactions. Results of chemical calculations can be influenced by solvation, which can push the simulation conditions toward the most stable form. However, the results for methotrexate connected to DWNTs are very significant, since they are highly consistent with the behavior of SWNTs and point to methanol and water as the most efficient solvents for this simulation. Given that performing calculations for molecular mechanics force fields requires selecting an appropriate force field in the beginning, the specifications of these 4 fields were closely investigated. Our choice was guided by force field equation for these fields and finally, we found that the MM+, which is an exclusive force field for calculations related to macromolecules had the lowest amount of energy and featured the most stable form of connection for methotrexate connected to SWNTs and DWNTs [67, 68].

Notably, in some solvents and at certain temperatures, the CHARMM force field demonstrates a similar behavior and puts our compound in a stable situation. However, since electrostatic reactions are calculated through bipolar junctions by using point charges in the MM+ field, the field managed to simulate our desired system in the most optimal way. Therefore, the MM+ force field was chosen as the most efficient field. It should further be noted that the results of quantum mechanics calculations are also consistent with the current findings and that DWNTs are more suitable carriers for methotrexate. The results of Monte Carlo, molecular mechanics and quantum mechanics calculations have been justified [69].

In macromolecules, thermodynamic parameters such as enthalpies, entropies, and free energies depend on many conformational degrees of freedom that these flexible molecules can take. We typically cannot estimate free energies of macromolecules in solutions using Monte Carlo simulations, partially because transitions from one conformer to another occur infrequently. Furthermore, for macromolecules molecular mechanics simulations frequently offer more efficient sampling of conformational space [70, 71].

What we can do with Monte Carlo or molecular dynamics simulations, however, is to estimate free energy differences between similar systems. Such calculations allow, for example, to compare binding

Table 1. Total (E_{Tot}), Potential (E_{Pot}), and Kinetic (E_{Kin}) energies (kcal/mol) calculated for the Native structure by Monte Carlo simulation in different solvents and AMBER force field for SWNTs with methotrexate.

Monte Carlo. AMBER											
Temperature		298K	300K	302K	304K	306K	308K	310K	312K	314K	316K
Gas (ε_r =1)	E_{Kin}	397.0588	399.7236	402.3884	405.0533	407.7181	410.3829	413.0477	415.7126	418.3774	421.0422
	E_{Pot}	1299774	115283.8	22806.42	5667.44	2184.987	1151.147	691.0261	461.2767	321.6936	228.879
	E_{Tot}	1300171	115683.5	23208.81	6072.494	2592.705	1561.53	1104.074	876.9892	740.071	649.9212
Water (ε_r =78.39)	E_{Kin}	1601.559	1612.308	1623.057	1633.805	1644.554	1655.303	1666.052	1676.8	1687.549	1698.298
	E_{Pot}	1284311	120491.7	32982.9	15263.81	10833.69	9004.202	7926.857	7152.551	6635.623	6316.146
	E_{Tot}	1285913	120104.1	34605.96	16897.61	12478.24	10659.51	9592.909	8829.352	8323.172	8014.444
Methanol (ε_r=32.63)	E_{Kin}	663.5412	667.9945	672.4478	676.9011	681.3544	685.8077	690.261	694.7143	699.1676	703.6209
	E_{Pot}	1683891	184554.1	44240.94	12638.16	5400.779	2833.486	1840.087	1377.098	959.6909	775.7297
	E_{Tot}	1684555	185222.1	44913.39	13315.06	6082.133	3519.294	2530.248	2011.812	1658.859	1479.351
Ethanol (ε_r =24.55)	E_{Kin}	796.7824	802.1299	807.4775	812.825	818.1725	823.5201	828.8676	834.2151	839.5627	844.9102
	E_{Pot}	2054430	248518.2	73643.34	23923.05	9969.078	5212.997	3265.047	2263.598	1739.065	1375.425
	E_{Tot}	2055227	249320.4	74450.82	24735.88	10787.25	6036.517	4093.915	3097.813	2578.628	2220.336
DMSO (ε_r =46.8)	E_{Kin}	841.1961	846.8417	852.4873	858.133	863.7786	869.4242	875.0698	880.7154	886.361	892.0066
	E_{Pot}	3234915	391200.3	139001.6	56097.66	21835.49	9763.858	5690.654	3846.583	2745.915	2110.565
	E_{Tot}	3235757	392047.1	139854.1	56955.8	22699.27	10633.28	6565.723	4727.299	3632.276	3002.572
DMF (ε_r =38.3)	E_{Kin}	878.5037	884.3997	890.2957	896.1917	902.0877	907.9836	913.8796	919.7756	925.6716	931.5676
	E_{Pot}	3431728	425782.3	161572.6	70387.31	31793.78	16393.95	10820.24	5742.012	2795.6	1994.713
	E_{Tot}	3432606	426666.7	162462.9	71283.5	32695.87	17301.93	11734.12	6661.787	3721.272	2926.281

Table 2. Total (E_{Tot}), Potential (E_{Pot}), and Kinetic (E_{Kin}) energies (kcal/mol) calculated for the Native structure by Monte Carlo simulation in different solvents and OPLS force field for SWNTs with methotrexate.

Monte Carlo. OPLS											
Temperature		298K	300K	302K	304K	306K	308K	310K	312K	314K	316K
Gas (ε_r =1)	E_{Kin}	210.5211	211.934	213.3469	214.7598	216.1727	217.5856	218.9985	220.4114	221.8242	223.2371
	E_{Pot}	4585.843	1424.573	937.0904	842.7628	782.4532	733.1329	720.3787	707.5767	682.9005	652.1961
	E_{Tot}	4796.364	1636.507	1150.437	1057.523	998.6259	950.7185	939.3771	927.9881	904.7247	875.4332
Water (ε_r =78.39)	E_{Kin}	1537.603	1547.923	1558.242	1568.562	1578.881	1589.201	1599.52	1609.84	1620.159	1630.479
	E_{Pot}	33741.44	3208.032	1568.416	836.1907	361.7393	-13.73618	-285.0799	-488.8704	-680.551	-867.092
	E_{Tot}	35279.04	4755.955	3126.659	2404.753	1940.621	1575.465	1314.44	1120.97	939.6083	763.3863
Methanol (ε_r =32.63)	E_{Kin}	477.0035	480.2049	483.4062	486.6076	489.809	493.0103	496.2117	499.4131	502.6144	505.8158
	E_{Pot}	124099	41566.57	21769.48	14609.36	12780.93	12221.92	11825.4	11589.35	11437.28	11353.56
	E_{Tot}	124576	42046.77	22252.89	15095.96	13270.74	12714.93	12321.61	12088.76	11939.89	11859.37
Ethanol (ε_r =24.55)	E_{Kin}	610.2447	614.3403	618.4359	622.5315	626.6271	630.7227	634.8183	638.9139	643.0095	647.1051
	E_{Pot}	317949.9	85433.54	44548.75	27906.72	20335.59	17559.04	15627.43	14419.03	13417.00	11817.21
	E_{Tot}	318560.1	86047.88	45167.18	28529.26	20962.22	18189.76	16262.25	15057.94	14060.00	12464.32
DMSO (ε_r =46.8)	E_{Kin}	654.6584	659.0521	663.4458	667.8395	672.2332	676.6268	681.0205	685.4142	689.8079	694.2016
	E_{Pot}	121998.1	36942.97	19157.97	13435.76	10908.04	9667.637	8992.501	8564.524	8328.571	8132.158
	E_{Tot}	122652.8	37602.02	19821.42	14103.6	11580.27	10344.26	9673.521	9249.938	9018.378	8826.36
DMF (ε_r =38.3)	E_{Kin}	743.4859	748.4757	753.4656	758.4554	763.4453	768.4351	773.4249	778.4148	783.4046	788.3945
	E_{Pot}	126576.2	44258.07	21382.49	14617.55	13004.05	12356.65	11925.29	11635.41	11405.72	11253.18
	E_{Tot}	127319.7	45006.54	22135.96	15376	13767.5	13125.08	12698.72	12413.83	12189.12	12041.58

affinities of similar drug molecules to the target receptor, thus facilitating rational design of more potent and selective drugs [72]. A word of caution is due here, however. Monte Carlo sampling of harmonic potential

Table 3. Total (E_{Tot}), Potential (E_{Pot}), and Kinetic (E_{Kin}) energies (kcal/mol) calculated for the Native structure by Monte Carlo simulation in different solvents and CHARMM force field for SWNTs with methotrexate.

Monte Carlo. CHARMM											
Temperature		298K	300K	302K	304K	306K	308K	310K	312K	314K	316K
Gas (ε_r =1)	E_{Kin}	210.5211	211.934	213.3469	214.7598	216.1727	217.5856	218.9985	220.4114	221.8242	223.2371
	E_{Pot}	3502.408	1195.034	856.0377	756.7777	706.5104	668.7651	643.4429	620.9258	607.4563	571.1967
	E_{Tot}	3712.929	1406.968	1069.385	971.5375	922.6831	886.3507	862.4414	841.3371	829.2805	794.4338
Water (ε_r =78.39)	E_{Kin}	1537.603	1547.923	1558.242	1568.562	1578.881	1589.201	1599.52	1609.84	1620.159	1630.479
	E_{Pot}	2167.736	-3391.008	-4206.12	-4507.294	-4638.172	-4704.273	-4799.169	-4932.309	-4972.38	-4970.701
	E_{Tot}	3705.34	-1843.085	-2647.878	-2938.732	-3059.291	-3115.072	-3199.648	-3322.469	-3352.22	-3340.222
Methanol (ε_r =32.63)	E_{Kin}	477.0035	480.2049	483.4062	486.6076	489.809	493.0103	496.2117	499.4131	502.6144	505.8158
	E_{Pot}	91945.87	35008.59	16778.84	12003.34	10510.41	9787.134	9362.204	9127.205	8932.238	8592.72
	E_{Tot}	92422.87	35488.8	17262.24	12489.95	11000.21	10280.14	9858.416	9626.618	9434.852	9098.536
Ethanol (ε_r =24.55)	E_{Kin}	610.2447	614.3403	618.4359	622.5315	626.6271	630.7227	634.8183	638.9139	643.0095	647.1051
	E_{Pot}	265655.2	70307.78	35446.18	21334.73	16740.28	14783.43	13513.86	12507.95	11403.35	10713.2
	E_{Tot}	266265.4	70922.12	36064.61	21957.26	17366.91	15414.16	14148.68	13146.86	12046.36	11360.31
DMSO (ε_r =46.8)	E_{Kin}	654.6584	659.0521	663.4458	667.8395	672.2332	676.6268	681.0205	685.4142	689.8079	694.2016
	E_{Pot}	170582.2	39843.12	20086.03	13775.94	11572.64	10399.47	9823.251	9434.371	9080.567	8736.918
	E_{Tot}	171236.9	40502.17	20749.48	14443.78	12244.88	11076.09	10504.27	10119.79	9770.375	9431.12
DMF (ε_r =38.3)	E_{Kin}	743.4859	748.4757	753.4656	758.4554	763.4453	768.4351	773.4249	778.4148	783.4046	788.3945
	E_{Pot}	103249.7	37293.97	21019.25	15074.97	13004.5	12350.34	11827.25	11477.62	11144.98	10867.57
	E_{Tot}	103993.2	38042.44	21772.71	15833.43	13767.94	13118.77	12600.68	12256.04	11928.39	11655.96

Table 4. Total (E_{Tot}), Potential (E_{Pot}), and Kinetic (E_{Kin}) energies (kcal/mol) calculated for the Native structure by Monte Carlo simulation in different solvents and MM+ force field for SWNTs with methotrexate.

Monte Carlo. MM+											
Temperature		298K	300K	302K	304K	306K	308K	310K	312K	314K	316K
Gas (ε_r =1)	E_{Kin}	210.5211	211.934	213.3469	214.7598	216.1727	217.5856	218.9985	220.4114	221.8242	223.2371
	E_{Pot}	1500.161	901.4761	761.6816	712.8203	634.4072	601.9166	577.8038	569.9135	555.8868	556.8354
	E_{Tot}	1710.682	1113.41	975.0285	927.5801	850.5799	819.5022	796.8022	790.3248	777.7111	780.0726
Water (ε_r =78.39)	E_{Kin}	1537.603	1547.923	1558.242	1568.562	1578.881	1589.201	1599.52	1609.84	1620.159	1630.479
	E_{Pot}	18254.24	11484.08	7683.593	5387.485	3839.653	3013.839	2323.27	2051.374	1738.824	1542.081
	E_{Tot}	19791.84	13032.01	9241.836	6956.047	5418.534	4603.04	3922.79	3661.214	3358.983	3172.56
Methanol (ε_r=32.63)	E_{Kin}	477.0035	480.2049	483.4062	486.6076	489.809	493.0103	496.2117	499.4131	502.6144	505.8158
	E_{Pot}	94358.97	72576.55	58611.3	48843.72	41821.43	36500.55	32412.08	28870.78	26080.32	23705.96
	E_{Tot}	94835.98	73056.76	59094.71	49330.33	42311.24	36993.56	32908.29	29370.19	26582.93	24211.78
Ethanol (ε_r=24.55)	E_{Kin}	610.2447	614.3403	618.4359	622.5315	626.6271	630.7227	634.8183	638.9139	643.0095	647.1051
	E_{Pot}	155252.2	120452.6	98101.16	83753.44	72193.42	63347.63	55520.07	49128.26	43928.58	39842.18
	E_{Tot}	155862.4	121066.9	98719.6	84375.97	72820.04	63978.35	56154.89	49767.17	44571.59	40489.28
DMSO (ε_r =46.8)	E_{Kin}	654.6584	659.0521	663.4458	667.8395	672.2332	676.6268	681.0205	685.4142	689.8079	694.2016
	E_{Pot}	112582.2	84122.59	66509.9	55302.35	46937.72	40828.36	36085.03	32008.44	28733.31	26215.18
	E_{Tot}	113236.8	84781.64	67173.35	55970.19	47609.96	41504.98	36766.05	32693.86	29423.12	26909.38
DMF (ε_r =38.3)	E_{Kin}	743.4859	748.4757	753.4656	758.4554	763.4453	768.4351	773.4249	778.4148	783.4046	788.3945
	E_{Pot}	79612.04	60252.73	48653.5	41296.18	36117.43	32031.92	28432.16	25607.77	23291.04	21318.94
	E_{Tot}	80355.53	61001.2	49406.96	42054.63	36880.87	32800.36	29205.59	26386.18	24074.45	22107.33

gives classical probability distributions, while bond vibrations in the real methotrexate anticancer drug atoms with carbon nanotube molecules are quantized. Consequently, classical Monte Carlo simulations fail to precisely reproduce such thermodynamic properties as heat capacities or vibrational entropies of isolated

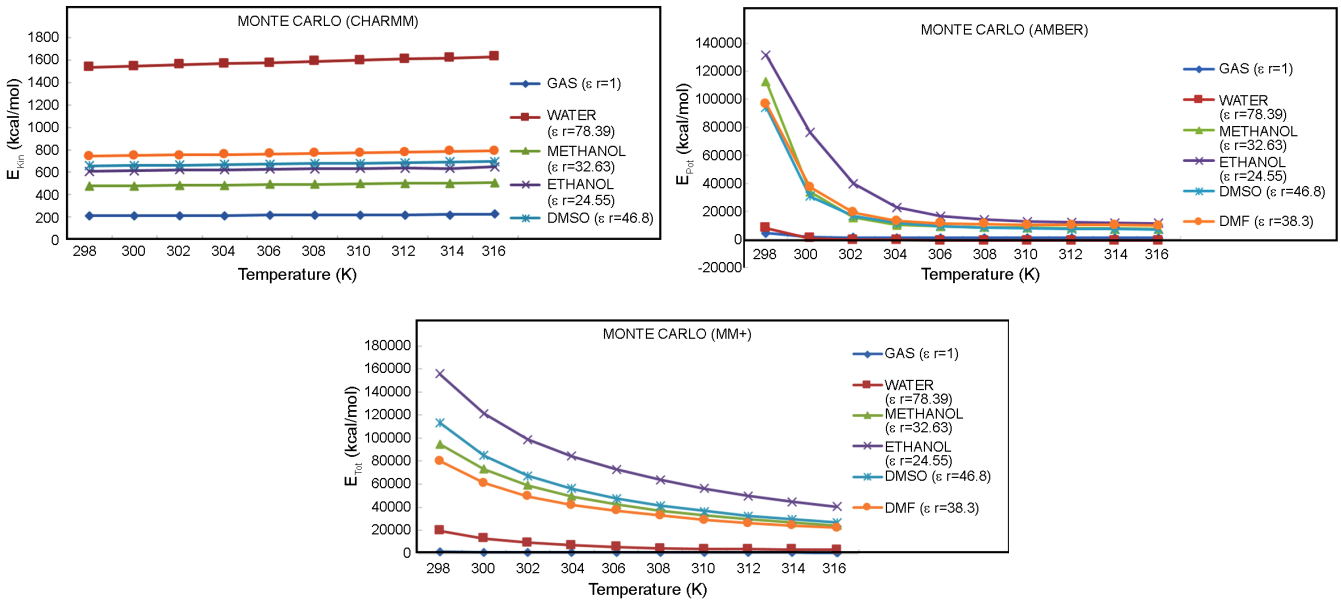

Fig. 1. E_{Kin}, E_{Pot} and E_{Tot} changes (kcal/mol) calculated versus temperature at different dielectric constants by Monte Carlo simulation in the CHARMM, AMBER and MM+ force field for SWNTs with methotrexate.

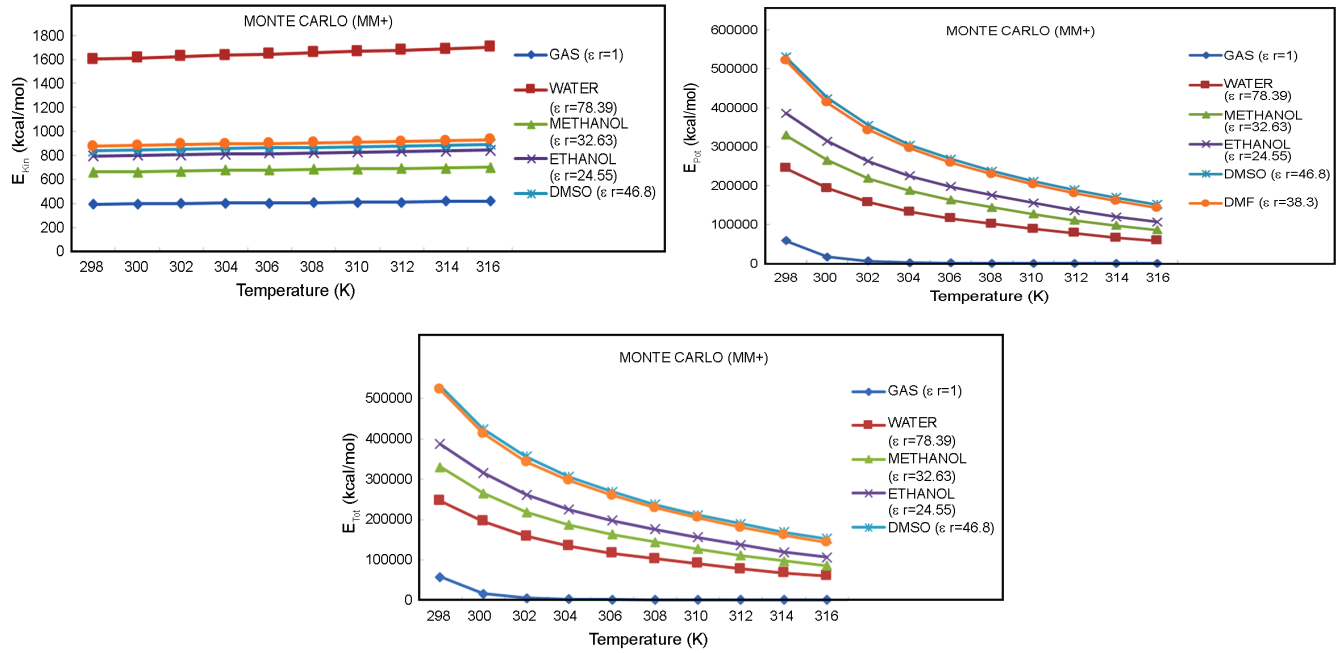

Fig. 2. E_{Kin}, E_{Pot} and E_{Tot} changes (kcal/mol) calculated versus temperature at different dielectric constants by Monte Carlo simulation in the MM+ force field for MWNTs with methotrexate.

molecules. Therefore, in this section we have used the quantum mechanics methods [73, 74].

Quantum chemical methods are important for obtaining information about molecular structure and electrochemical behavior. A frontier molecular orbitals (FMO) analysis was done for the compounds using the B3LYP/6-311+G(d) level [33]. FMO results such as E_{HOMO}, E_{LUMO} and the HOMO-LUMO energy gap (ΔE) of the title compounds have been summarized in Table 5. The energy of the LUMO, HOMO and their energy gaps reflect the chemical reactivity of the molecule [38]. In addition, the HOMO can act

as an electron donor and the LUMO as an electron acceptor. An increased level of HOMO energy (E_{HOMO}) for the molecule points to a heightened ability to donate electrons to a suitable acceptor molecule that has a low-energy empty molecular orbital. The E_{HOMO} and E_{LUMO} are related to the ionization potential ($I=-E_{HOMO}$) and the electron affinity ($A=-E_{LUMO}$), respectively [19, 21]. The global hardness (η), electronegativity (χ), electronic chemical potential (μ) and electrophilicity (ω) and chemical softness (S) parameters [16] are calculated with the following equations:

$$\left(\eta = I - A/2\right) \quad (1)$$

$$\left(\chi = I + A/2\right) \quad (2)$$

$$\left(\mu = -(I + A)/2\right) \quad (3)$$

$$\left(\omega = \mu^2/2\eta\right) \quad (4)$$

$$\left(s = 1/2\eta\right) \quad (5)$$

The values of these parameters are reported in Table 5. The global hardness (η) parameter is related to the energy gap ($Eg = E_{LUMO} - E_{HOMO}$) and defined as the resistance of an atom or a group of atoms to charge transfer. As shown in Table 5, the HOMO energy of the compound methotrexate with (SWNTs) has the highest value (-0.0204eV). A large energy gap implies high stability for the molecule. The HOMO–LUMO energy gap (ΔE) values calculated for the structures methotrexate with (SWNTs) and methotrexate with (DWNTs) are 0.018486 and 0.021495 eV, respectively. The results show that compound methotrexate with (DWNTs) is more stable. DOS plots [40] also demonstrate the energy gaps (ΔE) calculated for the methotrexate (see Fig. 3). Table 5 shows the specifics of quantum molecular descriptors of title compounds such as electron affinity, ionization potential, electronic chemical potential, global hardness and electrophilicity. The chemical hardness (η) values for the compounds methotrexate with (SWNTs) and methotrexate with (DWNTs) are 0.01927 eV and 0.022406 eV, respectively. Compound methotrexate with (DWNTs) has the highest chemical hardness (η = 0.022406 eV); therefore, it is a hard, less reactive molecule with a high energy gap (ΔE= 0.021495 eV).

A form of potential energy, electronic chemical potential (μ= -(I + A)/2) has the capacity to be absorbed or released during chemical reactions and might also be modified during phase transitions. The electronic chemical potential of methotrexate with (DWNTs) has the most negative value -0.012572 eV). Electrophilicity (ω) is a measure of energy stabilization for when the system receives an additional electronic charge from the environment. This index (ω= μ2/2η) holds information about both electron transfer (chemical potential) and stability (hardness); it also describes global chemical reactivity more precisely. The higher value of electrophilicity index shows the higher capacity of the molecule to accept electrons. The electrophilicity index for the methotrexate with (SWNTs) and methotrexate with (DWNTs) are 0.003032 and 0.003526 eV, respectively. Methotrexate with (DWNTs) has the highest electrophilicity index; therefore its capacity for accepting electrons is quite high. The dipole moment (μD) is an appropriate measure of the asymmetric nature of molecules. The composition and dimensionality of the 3D structures determine its magnitude. As shown in Table 5, all structures have a high value of dipole moment and point group of C1, which reflects no symmetry in the structures. The dipole moment for the methotrexate with (SWNTs) (B3LYP/6-31+G(d) = 2.8990 Debye) is higher than that for methotrexate with (DWNTs) (2.43746 Debye, respectively).

The asymmetric character of methotrexate with (SWNTs) is the reason behind its high dipole moment value [75, 76]. As presented in Table 5, the compound which have the lowest energetic gap is the methotrexate + (SWNTs) (Eg = 0.018486 eV). This lower gap allows it to be the softest molecule. The compound that have the highest energy gap is the methotrexate (Eg = 0.09243 eV). The compound that has the highest HOMO energy is the methotrexate (EHOMO = -0.10027 eV). This higher energy allows it to be the best electron donor. The compound that has the lowest LUMO energy is the methotrexate (E_{LUMO} = -0.00784 eV) which signifies that it can be the best electron acceptor.

The two properties like I (potential ionization) and A (affinity) are so important, the determination of these two properties allow us to calculate the absolute

Table 5. The calculated electronic properties of the methotrexate using B3LYP/6-31+G* level of theory.

Property	Methotrexate	Methotrexate + (SWNTs)	Methotrexate + (MWNTs)
HF (Hartree)	-1569.0359759	-8375.4696343	-6832.7643987
Zero-point correction (Hartree)	0.448736	0.0897472	0.1043572
Thermal correction to Energy (Hartree)	0.478604	0.0957208	0.1113032
Thermal correction to Enthalpy (Hartree)	0.479548	0.0959096	0.1115227
Thermal correction to Gibbs Free Energy (Hartree)	0.382959	0.0765918	0.0890602
Sum of electronic and zero-point Energies (Hartree)	-1568.587240	-313.717448	-364.7877302
Sum of electronic and thermal Energies (Hartree)	-1568.557372	-313.7114744	-364.7807841
Sum of electronic and thermal Enthalpies (Hartree)	-1568.556428	-313.7112856	-364.7805646
Sum of electronic and thermal Free Energies (Hartree)	-1568.653016	-313.7306032	-364.8030269
E (Thermal) (KCal.Mol)	300.329	60.0658	69.8439
CV (Cal.Mol-Kelvi)	112.873	22.5746	26.2495
S (Cal.Mol-Kelvin)	203.288	40.6576	47.2762
Dipole moment (Debye)	10.4811	2.8990	2.43746
Point Group	C1	C1	C1
E_{HOMO} (eV)	-0.10027	-0.020054	-0.023318
E_{LUMO} (eV)	-0.00784	-0.001568	-0.001823
Eg (eV)	0.09243	0.018486	0.021495
I (eV)	0.10027	0.020054	0.023318
A (eV)	0.00784	0.001568	0.001823
χ (eV)	0.10419	0.020838	0.024230
η (eV)	0.09635	0.01927	0.022406
μ (eV)	-0.05406	-0.01081	-0.012572
ω (eV)	0.015163	0.003032	0.003526
S (eV)	5.189414	1.037882	1.206840

electro negativity (χ) and the absolute hardness (η). These two parameters are related to the one-electron orbital energies of the HOMO and LUMO respectively. Methotrexate + (SWNTs) has lowest value of the potential ionization (I = 0.020054 eV), so that will be the better electron donor. Methotrexate has the largest value of the affinity (A = 0.00784eV), so it is the better electron acceptor. The chemical reactivity varies with the structural of molecules. Chemical hardness (softness) value of methotrexate (η = 0.09635 eV, S = 5.189414 eV) is lesser (greater) among all the molecules. Thus, methotrexate is found to be more reactive than all the compounds. Methotrexate + (MWNTs) possesses higher electro negativity value (χ = 0.024230 eV) than all compounds so; it is the best electron acceptor. The value of ω for methotrexate + (MWNTs) (ω = 0.003526 eV) indicates that it is the stronger electrophiles than all compounds. Compound 3 has the smaller frontier orbital gap so, it is more polarizable and is associated with a high chemical reactivity, low kinetic stability and is also termed as soft molecule.

The total energy of a molecule consists of the sum of translational, rotational, vibrational and electronic energies. The statistical thermochemical analysis of title compounds is carried out by placing the molecule at the room temperature of 25°C and under 1 atmospheric pressure. The thermodynamic parameters, such as zero point vibrational energy, rotational constant, heat capacity (C) and entropy (S) of the title compound by B3LYP/6-31+G(d) level are displayed in Table 5. According to this table, the calculated value for methotrexate with (DWNTs) is smaller than those for methotrexate with (SWNTs). The results suggest that compound methotrexate with (DWNTs) is more stable [77].

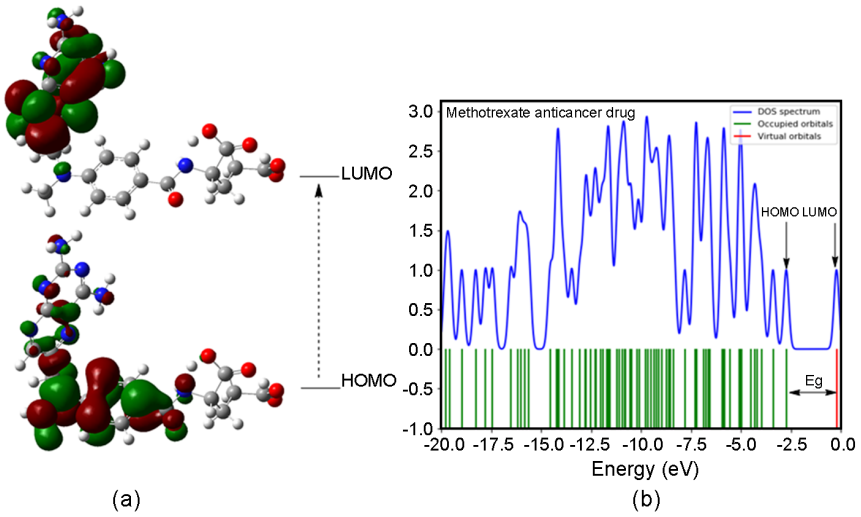

Fig. 3. (a) Calculated Frontier molecular orbitals of methotrexate (ΔE: energy gap between LUMO and HOMO), (b) Calculated DOS plots of the title compounds (using the B3LYP/6-31+G*).

Molecular electrostatic potential (MEP) calculations display the charge distribution and sites of negative and positive charges. The differences in the electrostatic potential on the surface are shown by different colors. The colors of the MEP maps are red (electron rich), orange (partially negative charge), yellow (slightly electron rich site), blue (positive charge or electron poor), and green (neutral). The MEP surfaces of molecule methotrexate were calculated by theoretical calculations using the B3LYP/6-31+G* level of theory (Fig. 4) [78]. As can be seen in Fig. 4, the negative sites (red color) of this molecule are mostly focused on oxygen atoms. Also, phenyl rings at the end of title compounds have a yellow color, indicating slightly electron rich sites. The hydrogen atoms of the methoxy group in the molecule are pale blue, which demonstrate regions with weak interaction. Also, the regions with green color show areas with zero potential and neutral sites such as the hydrogen atoms of the phenyl rings and carbon chains in substituted groups of the methotrexate [79].

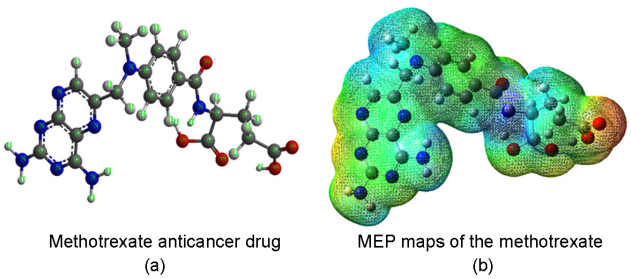

Fig. 4. (a) The theoretical geometric structure of the methotrexate anticancer drug (optimized by B3LYP/6-31+G level); (b). MEP maps of the methotrexate calculated using the B3LYP/6-31+G* level of theory.

CONCLUSIONS

Monte Carlo simulations have been of significant value in understanding the structure and characteristics of liquids. For example, Monte Carlo simulations with accurate energy potentials can estimate liquid densities and heats of vaporization with little percent accuracy. Monte Carlo simulations can provide information about the structure of hydration shells around solutes and allow estimations of how different solvents alter the energy profiles in chemical reactions. When methotrexate connected to SWNTs was simulated in water, DMSO, methanol, ethanol and DMF solvents, the methanol solvent had the lowest amount of energy and was the most stable solvent for the simulation. Similar results have been reported for OPLS and CHARMM force fields. However, the calculations related to the MM+ force field yielded a notable result. In the MM+ field, water is the most suitable solvent for simulation, since it has the lowest amount of energy and is therefore the most stable among the solvents mentioned above. The results for methotrexate connected to DWNTs, show that the results are

highly consistent with those related to methotrexate connected to SWNTs; in the force fields Amber, OPLS and CHARMM, methanol is the most stable solvent and in the MM+ field, water is the most stable solvent. However, the results for methotrexate connected to DWNTs are very significant, since they are highly consistent with the behavior of SWNTs and point to methanol and water as the most efficient solvents for this simulation.

Therefore, the MM+ force field was chosen as the most efficient field. The MM+ force field which is an exclusive force field for calculations related to macromolecules was found to have the lowest amount of energy and feature the most stable form of connection for methotrexate connected to SWNTs and DWNTs. It should further be noted that the results of quantum mechanics calculations are also consistent with the current findings and that DWNTs are more suitable carriers for methotrexate.

Delivering anti-cancer drugs through SWCNTs and MWCNTs is a considerable breakthrough in the field of nanotechnology. Conventional management of cancer with chemotherapeutic agents can have adverse effects on healthy tissues. Therefore, CNTs -based efficient drug delivery systems must be developed to deliver the anti-cancer drugs. Even though nano-technology is well developed, it is still far from clinical applications due to several challenges. However, SWCNTs and MWCNT-based drug delivery systems are promising approaches for delivering anti-cancer drugs in targeted organs or tissues. The observation and results of this review paper indicated that SWCNTs and MWCNT-based drug delivery systems might be effective and able to provide adequate scientific data for clinical support.

CONFLICTS OF INTEREST

The authors declare no conflicts of interest.

DECLARATION OF FUNDING

This research did not receive any specific funding.

AVAILABILITY OF DATA

The data that support this study are available in the article and accompanying online supplementary material.

ACKNOWLEDGEMENT

The authors are thankful to the Ahvaz Branch of Islamic Azad University and the Zanjan Branch of Islamic Azad University for partial support of this work.

REFRENCES

[1] Li, X.; Peng, Y.; Qu, X. (2006). Carbon nanotubes selective destabilization of duplex and triplex DNA and inducing B–A transition in solution. Nucleic Acids Res., 34, 3670-3676.

[2] Klumpp, C.; Kostarelos, K.; Prato, M.; Bianco, A., (2006). Functionalized carbon nanotubes as emerging nanovectors for the delivery of therapeutics. Biochimica et Biophysica Acta (BBA)-Biomembranes, 1758, 404-412.

[3] Sinha, N.; Yeow, J.-W. (2005). Carbon nanotubes for biomedical applications. IEEE Trans. Nanobiosci., 4, 180-195.

[4] Nishiyama, N.; Kataoka, K. (2006). Current state, achievements, and future prospects of polymeric micelles as nanocarriers for drug and gene delivery. Pharmacol. Ther., 112, 630-648.

[5] Mizusako, H.; Tagami, T.; Hattori, K.; Ozeki, T. (2015). Active drug targeting of a folate-based cyclodextrin–doxorubicin conjugate and the cytotoxic effect on drug-resistant mammary tumor cells in vitro. J. Pharm. Sci., 104, 2934-2940.

[6] He, Q.; Shi, J. (2011). Mesoporous silica nanoparticle based nano drug delivery systems: synthesis, controlled drug release and delivery, pharmacokinetics and biocompatibility. J. Mater. Chem., 21, 5845-5855.

[7] Kwon, G.; Suwa, S.; Yokoyama, M.; Okano, T.; Sakurai, Y.; Kataoka, K. (1994). Enhanced tumor accumulation and prolonged circulation times of micelle-forming poly (ethylene oxide-aspartate) block copolymer-adriamycin conjugates. J. Controlled Release, 29, 17-23.

[8] Mahmud, A.; Xiong, X.-B.; Aliabadi, H. M.; Lavasanifar, A. (2007). Polymeric micelles for drug targeting. J. Drug Target., 15, 553-584.

[9] Khatri, S.; Das, N. G.; Das, S. K. (2014). Effect of methotrexate conjugated PAMAM dendrimers on

the viability of MES-SA uterine cancer cells. J. Pharm. Bioallied Sci., 6, 297.

[10] Kim, J.-E.; Shin, J.-Y.; Cho, M.-H. (2012). Magnetic nanoparticles: an update of application for drug delivery and possible toxic effects. Arch. Toxicol., 86, 685-700.

[11] Sun, C.; Lee, J. S.; Zhang, M. (2008). Magnetic nanoparticles in MR imaging and drug delivery. Adv. Drug Delivery Rev., 60, 1252-1265.

[12] Binenbaum, Y.; Na'ara, S.; Gil, Z. (2015). Gemcitabine resistance in pancreatic ductal adenocarcinoma. Drug Resistance Updates, 23, 55-68.

[13] Tyagi, N.; Song, Y. H.; De, R. (2019). Recent progress on biocompatible nanocarrier-based genistein delivery systems in cancer therapy. J. Drug Target., 27, 394-407.

[14] Uchegbu, I. F.; Schatzlein, A. G. (2006). Polymers in drug delivery.CRC Press.

[15] Johnston, A.; Gudjonsson, J. E.; Sigmundsdottir, H.; Ludviksson, B. R.; Valdimarsson, H. (2005). The anti-inflammatory action of methotrexate is not mediated by lymphocyte apoptosis, but by the suppression of activation and adhesion molecules. Clinical Immunology, 114, 154-163.

[16] Meyer, L. M.; Miller, F. R.; Rowen, M. J.; Bock, G.; Rutzky, J. (1950). Treatment of acute leukemia with amethopterin (4-amino, 10-methyl pteroyl glutamic acid). Acta haematologica, 4, 157-167.

[17] Mol, F.; Mol, B.; Ankum, W.; Van der Veen, F.; Hajenius, P. (2008). Current evidence on surgery, systemic methotrexate and expectant management in the treatment of tubal ectopic pregnancy: a systematic review and meta-analysis. Human reproduction update, 14, 309-319.

[18] Rajagopalan, P. R.; Zhang, Z.; McCourt, L.; Dwyer, M.; Benkovic, S. J.; Hammes, G. G. (2002). Interaction of dihydrofolate reductase with methotrexate: ensemble and single-molecule kinetics. Proc. Natl. Acad. Sci. U.S.A, 99, 13481-13486.

[19] Scheinfeld, N. (2006). Genital warts. Dermatol. Online J., 12.

[20] Cronstein, B. N. (2005). Low-dose methotrexate: a mainstay in the treatment of rheumatoid arthritis. Pharmacol. Rev., 57, 163-172.

[21] Sawaya, M.; Kraut, J. (1997). Loop and Subdomain Movements in the Mechanism of Escherichia coli Dihydrofolate Reductase: Crystallographic Evidence. Biochemistry, 36, 586− 603.

[22] Fierke, C. A.; Johnson, K. A.; Benkovic, S. J. (1987). Construction and evaluation of the kinetic scheme associated with dihydrofolate reductase from Escherichia coli. Biochemistry, 26, 4085-4092.

[23] Cameron, C. E.; Benkovic, S. J. (1997). Evidence for a functional role of the dynamics of glycine-121 of Escherichia coli dihydrofolate reductase obtained from kinetic analysis of a site-directed mutant. Biochemistry, 36, 15792-15800.

[24] Beckett, D.; Kovaleva, E.; Schatz, P. J. (1999). A minimal peptide substrate in biotin holoenzyme synthetase-catalyzed biotinylation. Protein Sci. 1999, 8, 921-929.

[25] Miller, G. P.; Wahnon, D. C.; Benkovic, S. J. (2001). Interloop contacts modulate ligand cycling during catalysis by Escherichia coli dihydrofolate reductase. Biochemistry, 40, 867-875.

[26] Dinnes, J.; Cave, C.; Huang, S.; Major, K.; Milne, R., (2001). The effectiveness and cost-effectiveness of temozolomide for the treatment of recurrent malignant glioma: a rapid and systematic review. Database of Abstracts of Reviews of Effects (DARE): Quality-assessed Reviews, 2001.

[27] O'Brien, F. J.; Harley, B.; Yannas, I. V.; Gibson, L. J. (2005). The effect of pore size on cell adhesion in collagen-GAG scaffolds. Biomaterials, 26, 433-441.

[28] Champion, J. A.; Mitragotri, S. (2006). Role of target geometry in phagocytosis. Proc. Natl. Acad. Sci. U.S.A, 103, 4930-4934.

[29] Piryaei, F.; Shajari, N.; Yahyaei, H. (2020). Efficient ZrO(NO3) 2.2 H2O catalyzed synthesis of 1H-indazolo [1, 2-b] phthalazine-1, 6, 11 (13H)-triones and electronic properties analyses, vibrational frequencies, NMR chemical shift analysis, MEP: A DFT study. Heteroat. Chem, 2020.

[30] Kinnings, S. L.; Liu, N.; Buchmeier, N.; Tonge, P. J.; Xie, L.; Bourne, P. E. (2009). Drug discovery using chemical systems biology: repositioning the safe medicine Comtan to treat multi-drug and extensively drug resistant tuberculosis. PLoS Comput. Biol., 5, e1000423.

[31] Ekins, S.; Mestres, J.; Testa, B. (2007). In silico pharmacology for drug discovery: applications to targets and beyond. Br. J. Pharmacol., 152, 21-37.

[32] Fraenkel, L.; Nowell, W. B.; Michel, G.; Wiedmeyer, C. (2018). Preference phenotypes to facilitate shared decision-making in rheumatoid arthritis. Annals of the rheumatic diseases, 77, 678-683.

[33] Mathews, A. L.; Coleska, A.; Burns, P. B.; Chung, K. C. (2016). Evolution of patient decision-making regarding medical treatment of rheumatoid arthritis. Arthritis care & research, 68, 318-324.

[34] Workman, P. (2005). Drugging the cancer kinome: progress and challenges in developing personalized molecular cancer therapeutics. in Cold Spring Harbor symposia on quantitative biology. Cold Spring Harbor Laboratory Press.

[35] Collins, I.; Workman, P. (2006). New approaches to molecular cancer therapeutics. Nat. Chem. Biol., 2, 689-700.

[36] MacKerell Jr, A. D.; Bashford, D.; Bellott, M.; Dunbrack Jr, R. L.; Evanseck, J. D.; Field, M. J.; Fischer, S.; Gao, J.; Guo, H.; Ha, S. (1998). All-atom empirical potential for molecular modeling and dynamics studies of proteins. J. Phys. Chem. B, 102, 3586-3616.

[37] Mackerell Jr, A. D.; Feig, M.; Brooks III, C. L. (2004). Extending the treatment of backbone energetics in protein force fields: limitations of gas-phase quantum mechanics in reproducing protein conformational distributions in molecular dynamics simulations. J. Comput. Chem., 25, 1400-1415.

[38] Jorgensen, W. L.; Maxwell, D. S.; Tirado-Rives, J. (1996). Development and testing of the OPLS all-atom force field on conformational energetics and properties of organic liquids. J. Amer. Chem. Soc., 118, 11225-11236.

[39] Hornak, V.; Abel, R.; Okur, A.; Strockbine, B.; Roitberg, A.; Simmerling, C. (2006). Comparison of multiple Amber force fields and development of improved protein backbone parameters. Proteins Struct. Funct. Bioinf., 65, 712-725.

[40] Yahyaei, H.; Monajjemi, M.; Aghaie, H.; Zare, K. (2013). Monte Carlo quantum calculation for double-walled carbon nanotubes (DWNTs) combined to calixarene. J. Comput. Theor. Nanosci., 10, 2332-2341.

[41] Release, H. (2001). HyperCube. Inc., http://www.hyper. com.

[42] Panagiotopoulos, A. Z.; Quirke, N.; Stapleton, M.; Tildesley, D. (1988). Phase equilibria by simulation in the Gibbs ensemble: alternative derivation, generalization and application to mixture and membrane equilibria. Mol. Phys., 63, 527-545.

[43] Panagiotopoulos, A. Z. (1987). Direct determination of phase coexistence properties of fluids by Monte Carlo simulation in a new ensemble. Mol. Phys., 61, 813-826.

[44] Frenkel, D.; Smit, B. (2002). Understanding molecular simulation 2nd edition, Academic Press, London, UK.

[45] Matito-Martos, I.; Álvarez-Ossorio, J.; Gutiérrez-Sevillano, J.; Doblaré, M.; Martin-Calvo, A.; Calero, S. (2015). Zeolites for the selective adsorption of sulfur hexafluoride. Physical Chemistry Chemical Physics, 17, 18121-18130.

[46] Frisch, M.; Trucks, G.; Schlegel, H.; Scuseria, G.; Robb, M.; Cheeseman, J.; Scalmani, G.; Barone, V.; Mennucci, B.; Petersson, G. (2009). Gaussian 09; Gaussian, Inc. Wallingford, CT, 32, 5648-5652.

[47] Frisch, A.; Nielson, A.; Holder, A. (2000). Gaussview user manual. Gaussian Inc., Pittsburgh, PA, 556.

[48] Becke, A. D. (1993). Becke's three parameter hybrid method using the LYP correlation functional. J. Chem. Phys., 98, 5648-5652.

[49] Tomasi, J.; Mennucci, B.; Cammi, R. (2005). Quantum mechanical continuum solvation models. Chem. Rev., 105, 2999-3094.

[50] Yahyaei, H.; Sharifi, S.; Shahab, S.; Sheikhi, M.; Ahmadianarog, M. (2021). Theoretical study of adsorption of solriamfetol drug on surface of the B12N12 fullerene: a DFT/TD-DFT approach. Lett. Org. Chem., 18, 115-127.

[51] Szczepanska, A.; Espartero, J. L.; Moreno-Vargas, A. J.; Carmona, A. T.; Robina, I.; Remmert, S.; Parish, C. (2007). Synthesis and conformational analysis of novel trimeric maleimide cross-linking reagents. J. Org. Chem., 72, 6776-6785.

[52] Metropolis, N.; Rosenbluth, A. W.; Rosenbluth, M. N.; Teller, A. H.; Teller, E. (1953). Equation of state calculations by fast computing machines. J. Chem. Phys., 21, 1087-1092.

[53] Tang, L.; Li, J.; Zhao, Q.; Pan, T.; Zhong, H.; Wang, W. (2021). Advanced and Innovative Nano-Systems for Anticancer Targeted Drug Delivery. Pharmaceutics, 13, 1151.

[54] Bobrowska, D. M.; Olejnik, P.; Echegoyen, L.; Plonska-Brzezinska, M. E. (2019). Onion-like carbon nanostructures: An overview of bio-applications. Curr. Med. Chem., 26, 6896-6914.

[55] Anaya-Plaza, E.; Shaukat, A.; Lehtonen, I.; Kostiainen, M. A. (2021). Biomolecule-Directed Carbon Nanotube Self-Assembly. Adv. health mater., 10, 2001162.

[56] Ahlawat, J.; Asil, S. M.; Barroso, G. G.; Nurunnabi, M.; Narayan, M. (2021). Application of carbon nano onions in the biomedical field: Recent advances and challenges. Biomater. Sci., 9, 626-644.

[57] Yeh, Y.-T.; Gulino, K.; Zhang, Y.; Sabestien, A.; Chou, T.-W.; Zhou, B.; Lin, Z.; Albert, I.; Lu, H.; Swaminathan, V., (2020). A rapid and label-free platform for virus capture and identification from clinical samples. Proc. Natl. Acad. Sci. U.S.A, 117, 895-901.

[58] Klochkov, S. G.; Neganova, M. E.; Nikolenko, V. N.; Chen, K.; Somasundaram, S. G.; Kirkland, C. E.; Aliev, G. (2021). Implications of nanotechnology for the treatment of cancer: Recent advances. in Seminars in cancer biology. Elsevier.

[59] Evans, D. B. (2020). Commentary: Surgery for locally advanced pancreatic cancer after neoadjuvant therapy. Surgery.

[60] Gote, V.; Nookala, A. R.; Bolla, P. K.; Pal, D., (2021). Drug resistance in metastatic breast cancer: tumor targeted nanomedicine to the rescue. Int. J. mol. sci., 22, 4673.

[61] Liu, H.; Mei, Y.; Zhao, Q.; Zhang, A.; Tang, L.; Gao, H.; Wang, W. (2021). Black phosphorus, an emerging versatile nanoplatform for cancer immunotherapy. Pharmaceutics, 13, 1344.

[62] Mei, Y.; Tang, L.; Xiao, Q.; Zhang, Z.; Zhang, Z.; Zang, J.; Zhou, J.; Wang, Y.; Wang, W.; Ren, M. (2021). Reconstituted high density lipoprotein (rHDL), a versatile drug delivery nanoplatform for tumor targeted therapy. J. Mater. Chem. B, 9, 612-633.

[63] Liu, X.; Ying, Y.; Ping, J. (2020). Structure, synthesis, and sensing applications of single-walled carbon nanohorns. Biosens. Bioelectron., 167, 112495.

[64] Eskandari, P.; Abousalman-Rezvani, Z.; Roghani-Mamaqani, H.; Salami-Kalajahi, M. (2021). Polymer-functionalization of carbon nanotube by in situ conventional and controlled radical polymerizations. Adv. Colloid Interface Sci., 294, 102471.

[65] Bartkowski, M.; Giordani, S. (2021). Carbon nano-onions as potential nanocarriers for drug delivery. Dalton Transactions, 50, 2300-2309.

[66] Goscianska, J.; Olejnik, A.; Ejsmont, A.; Galarda, A.; Wuttke, S. (2021). Overcoming the paracetamol dose challenge with wrinkled mesoporous carbon spheres. J. Colloid Interface Sci., 586, 673-682.

[67] González-Domínguez, J. M.; Grasa, L.; Frontiñán-Rubio, J.; Abás, E.; Domínguez-Alfaro, A.; Mesonero, J. E.; Criado, A.; Ansón-Casaos, A. (2022). Intrinsic and selective activity of functionalized carbon nanotube/nanocellulose platforms against colon cancer cells. Colloids Surf. B: Biointerfaces, 212, 112363.

[68] Vallan, L.; Hernández-Ferrer, J.; Grasa, L.; González-Domínguez, J. M.; Martínez, M. T.; Ballesteros, B.; Urriolabeitia, E. P.; Ansón-Casaos, A.; Benito, A. M.; Maser, W. K. (2020). Differential properties and effects of fluorescent carbon nanoparticles towards intestinal theranostics. Colloids Surf. B: Biointerfaces, 185, 110612.

[69] Rezaei-Sameti, M.; Shiravand, E. (2020). The thermodynamic, quantum, AIM and NBO study of the interaction of pyrazinamide drug with the pristine and transition metal-doped B12P12. Adsorption, 26, 955-970.

[70] Akter, S.; Yamamoto, Y.; Zope, R. R.; Baruah, T. (2021). Static dipole polarizabilities of polyacenes using self-interaction-corrected density functional approximations. J. Chem. Phys., 154, 114305.

[71] Vargas, J.; Ufondu, P.; Baruah, T.; Yamamoto, Y.;

Jackson, K. A.; Zope, R. R. (2020). Importance of self-interaction-error removal in density functional calculations on water cluster anions. Phys. Chem. Chem. Phys., 22, 3789-3799.

[72] Akter, S.; Yamamoto, Y.; Diaz, C. M.; Jackson, K. A.; Zope, R. R.; Baruah, T. (2020). Study of self-interaction errors in density functional predictions of dipole polarizabilities and ionization energies of water clusters using Perdew–Zunger and locally scaled self-interaction corrected methods. J. Chem. Phys., 153, 164304.

[73] Narayanankutty, A.; Job, J. T.; Narayanankutty, V. (2019). Glutathione, an antioxidant tripeptide: dual roles in carcinogenesis and chemoprevention. Curr. Protein Peptide Sci., 20, 907-917.

[74] Shaaban, S.; Ferjani, H.; Althagafi, I.; Yousef, T. (2021). Crystal structure, Hirshfeld surface analysis, and DFT calculations of methyl (Z)-4-((4-((4-bromobenzyl) selanyl) phenyl) amino)-4-oxobut-2-enoate. J. Mol. Struct., 1245, 131072.

[75] Shaaban, S.; Zarrouk, A.; Vervandier-Fasseur, D.; Al-Faiyz, Y. S.; El-Sawy, H.; Althagafi, I.; Andreoletti, P.; Cherkaoui-Malki, M. (2021). Cytoprotective organoselenium compounds for oligodendrocytes. Arab. J. Chem., 14, 103051.

[76] Singh, J.; Khan, M.; Uddin, S. (2022). A DFT study of vibrational spectra of 5-chlorouracil with molecular structure, HOMO–LUMO, MEPs/ESPs and thermodynamic properties. Polym. Bull., 1-29.

[77] Pankin, D.; Martynova, N.; Smirnov, M.; Manshina, A. (2021). Spectral properties of triphenyltin chloride toxin and its detectivity by SERS: Theory and experiment. Spectrochim. Acta A Mol. Biomol. Spectrosc., 245, 118933.

[78] Jiang, S.; Chang, L.; Luo, J.; Zhang, J.; Liu, X.; Lee, C.-Y.; Zhang, W. (2021). Fabrication of a honeycomb-like bimetallic SERS substrate for the detection of triphenyltin chloride. Analyst, 146, 6170-6177.

[79] Pankin, D.; Smirnov, M.; Povolotckaia, A.; Povolotskiy, A.; Borisov, E.; Moskovskiy, M.; Gulyaev, A.; Gerasimenko, S.; Aksenov, A.; Litvinov, M. (2022). DFT Modelling of Molecular Structure, Vibrational and UV-Vis Absorption Spectra of T-2 Toxin and 3-Deacetylcalonectrin. Materials, 15, 649.

AUTHOR (S) BIOSKETCHES

Vahid Khodadadi, Ph.D., Department of Chemistry, Ahvaz Branch, Islamic Azad University, Ahvaz, Iran

Neda hasanzadeh, Assistant Professor, Department of Chemistry, Ahvaz Branch, Islamic Azad University, Ahvaz, Iran

Hooriye Yahyaei, Assistant Professor, Department of Chemistry, Zanjan Branch, Islamic Azad University, Zanjan, Iran, Email: Hooriye_Yahyaei@yahoo.com

Aye Rayatzadeh, Assistant Professor, Department of Chemistry, Ahvaz Branch, Islamic Azad University, Ahvaz, Iran